Compression-induced changes in the physiological state of the breast as observed through frequency domain photon migration measurements

Stefan A. Carp
Tina Kauffman
Qianqian Fang
Harvard Medical School
Massachusetts General Hospital
Athinoula A. Martinos Center for Biomedical Imaging
Charlestown, Massachusetts 02129

Elizabeth Rafferty
Richard Moore
Daniel Kopans
Harvard Medical School
Massachusetts General Hospital
Department of Radiology
Boston, Massachusetts 02114

David Boas
Harvard Medical School
Massachusetts General Hospital
Athinoula A. Martinos Center for Biomedical Imaging
Charlestown, Massachusetts 02129

Abstract. We use optical spectroscopy to characterize the influence of mammographic-like compression on the physiology of the breast. We note a reduction in total hemoglobin content, tissue oxygen saturation, and optical scattering under compression. We also note a hyperemic effect during repeated compression cycles. By modeling the time course of the tissue oxygen saturation, we are able to obtain estimates for the volumetric blood flow (1.64 ± 0.6 mL/100 mL/min) and the oxygen consumption (1.97 ± 0.6 μmol/100 mL/min) of compressed breast tissue. These values are comparable to estimates obtained from previously published positron emission tomography (PET) measurements. We conclude that compression-induced changes in breast physiological properties are significant and should be accounted for when performing optical breast imaging. Additionally, the dynamic characteristics of the changes in breast physiological parameters, together with the ability to probe the tissue metabolic state, may prove useful for breast cancer detection. [DOI: 10.1117/1.2397572]

Keywords: spectroscopy; mammography; frequency domain; photon migration; breast cancer; oxygen consumption; blood flow; mammographic compression; diffuse reflection.

Paper 06104R received Apr. 18, 2006; revised manuscript received Jul. 28, 2006; accepted for publication Aug. 1, 2006; published online Dec. 18, 2006.

1 Introduction

Optical imaging is a rapidly evolving imaging modality with potential clinical impact for detecting and diagnosing breast cancer.[1–4] Diffuse optical spectroscopy provides quantitative functional information based on the absorption and scattering properties of tissue that complements well high-resolution anatomical information obtained from radiographic methods. Tissue parameters derived from optical measurements include the concentration of oxy and deoxyhemoglobin (HbR and HbO), lipid and water, as well as the tissue hemoglobin oxygen saturation (S_tO_2). These parameters correlate with cancer pathological markers such as angiogenesis, hypoxia, and edema.[5]

Our group has developed a multimodality instrument that performs simultaneous diffuse optical tomography with x-ray tomosynthesis, and has obtained some promising initial results in imaging angiogenesis related to large breast tumors.[6] One notable feature of this system is that optical imaging is performed under mammographic compression. Jiang et al.[7] studied the effect of applying circumferential compression on the breast and found increases in both the total hemoglobin concentration and optical scattering while water content decreased. However, due to significant differences in measurement geometry as well as much lower applied pressures, it is not obvious how their results apply to our imaging system. Thus, we performed a pilot study to assess the change in the physiological parameters of the breast under mammographic-like compression and to also look for dynamic features that could allow us to enhance the diagnostic ability of our optical imaging system. For this purpose, we have recruited 56 healthy volunteers and we have measured the concentration of the hemoglobin species at various compression levels using a frequency domain spectrometer (ISS, Incorporated, Champaign, Illinois) in a same-side reflective configuration. We have also developed an algorithm for extracting the tissue oxygen consumption and volumetric blood flow from the transient changes in hemoglobin oxygen saturation, and we include data for select volunteers. We believe these quantities could become useful biomarkers for the presence of breast cancer.

2 Materials and Methods

2.1 *Experimental Design*

Figure 1 shows a schematic of the breast compression spectroscopy system. A computer-controlled translation stage applies between 0 and 12 lbs of compression to the subject's breast by means of two plastic compression plates. The upper plate is attached to the translation stage by means of two

Address all correspondence to Stefan Carp, Athinoula Martinos Center for Biological Imaging, Massachusetts General Hospital, 13th Street, Bldg 149, Room 2301, Charlestown, MA 02129, United States of America; Tel: 617-726-9332; Fax: 617-726-7422; E-mail: carp@nmr.mgh.harvard.edu

1083-3668/2006/11(6)/064016/6/$22.00 © 2006 SPIE

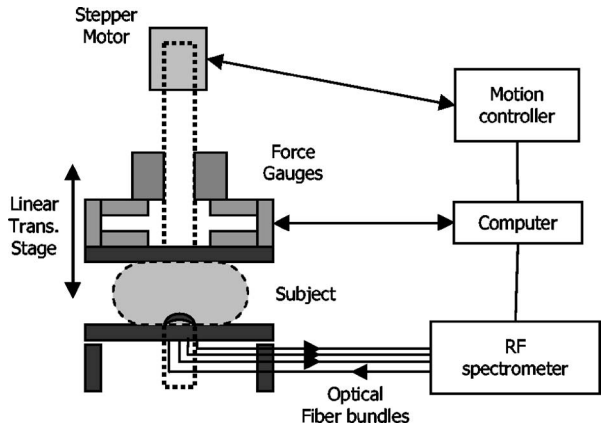

Fig. 1 Experimental setup. A computer-controlled translation stage applies compression to a subject's breasts while frequency domain optical measurements are acquired through one source and three detector fibers. Force transducers are integrated into the compression frame for monitoring.

strain gages to allow force measurement, while the lower plate is table mounted on a support, and contains the various light delivery and collection fibers.

The near-infrared measurements were performed with a frequency-domain tissue spectrometer (model 96208, ISS, Champaign, Illinois). This instrument uses four parallel photomultiplier tube detectors that are time shared by eight multiplexed laser diodes emitting at 635, 670, 691, 752, 758, 782, 811, and 831 nm, respectively. The frequency of intensity modulation is 110 MHz, and heterodyne detection is performed with a cross-correlation frequency of 5 kHz. A complete acquisition cycle over the eight wavelengths is completed every 80 ms. The laser diodes and the photomultiplier tubes are all coupled to fiber optics. The eight individual illumination fibers, each 400 μm in internal diameter, are arranged into a fiber bundle having a rectangular cross section of 3.5×2.0 mm^2. The collecting circular fiber bundles are 3.0 mm in internal diameter. The optical fibers are placed in contact with the breast by means of a plastic plate. As shown in Fig. 2, the tips of the illuminating and collecting fiber bundles are arranged along a line, 1.5 cm from the edge of the plate, with three collecting fiber bundles at distances of 1.5, 2.0, and 2.6 cm from the single illuminating bundle.

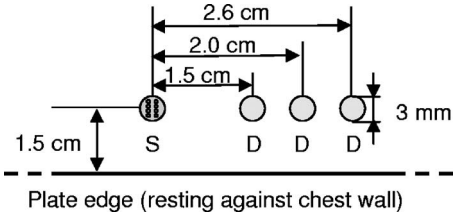

Fig. 2 Optical probe. The detector fiber bundles (D) are placed 1.5, 2.0, and 2.6 cm away from the source fiber bundle (S, individual fibers shown as tiny circles), respectively. All fibers are arranged in a line parallel to the edge of the bottom plate of the compression system, approximately 1.5 cm away from the chest wall.

2.2 *Human Subject Protocol*

Our Institutional Review Board (IRB) approved protocol called for the volunteer's breast to be placed in contact with the lower plate of the compression system with her chest wall resting against the edge of the plate. The upper plate is then brought down until it just makes contact with the breast. Baseline optical properties are recorded for 30 to 90 s, then 3 lbs of force are applied and the position is held for 30 s, after which the force is increased to 6 lbs and the optical properties are acquired for another 30 to 90 s. The upper plate is then moved up until all compression has been released and the entire cycle is repeated a total of 3 to 5 times. If the subject agreed, a four-step cycle was also used, containing 0-, 3-, 6-, and 12-lbs force plateaus (holding for 10 s at each force level) to more closely simulate the effects of mammographic compression (generally quoted to equal approximately 20 lbs of force). We chose these lower compression levels instead of full mammographic compression to improve subject compliance/accrual. Subjects were selected among healthy volunteers, more than 21 years old, with no open wounds on breast, breast implants, or breast biopsy within 3 months prior to participation in the study. The age range was 22 to 60 years old with an average of 30 years of age and standard deviation of 10 years.

2.3 *Spectroscopy Data Processing*

The tissue optical absorption (μ_a) and scattering (μ_s') coefficients are derived from the frequency domain measurements using a multidistance fitting algorithm as described in Refs. 8 and 9. The dependence on the source detector separation of the measured DC and AC components ($I_{\mathrm{DC}}, I_{\mathrm{AC}}$) as well as the phase ($\varphi$) of the diffusely reflected light is predicted by diffusion theory as follows:[9]

$$\ln(r^2 I_{\mathrm{DC}}) = rS_{\mathrm{DC}}(\mu_a, \mu_s') + C_{\mathrm{DC}}, \tag{1}$$

$$\ln(r^2 I_{\mathrm{AC}}) = rS_{\mathrm{AC}}(\mu_a, \mu_s') + C_{\mathrm{AC}}, \tag{2}$$

$$\varphi = rS_{\varphi}(\mu_a, \mu_s') + C_{\varphi}, \tag{3}$$

where S_{DC}, S_{AC}, and S_{φ} are the slopes characterizing the relationship between the source-detector separation r and $\ln(r^2 I_{\mathrm{DC}})$, $\ln(r^2 I_{\mathrm{AC}})$, and φ, respectively. C_{DC}, C_{AC}, and C_{φ} are constants independent of r. Again, from diffusion theory (if $r\sqrt{3\mu_a\mu_s'} \gg 1$):[8]

$$\mu_a = \frac{\omega}{2c_t}\left(\frac{S_{\varphi}}{S_{AC}} - \frac{S_{AC}}{S_{\varphi}}\right), \tag{4}$$

$$\mu_s' = \frac{S_{AC}^2 - S_{\varphi}^2}{3\mu_a} - \mu_a, \tag{5}$$

where ω is the modulation frequency of the light sources and c_t is the speed of light in tissue. The $\mu_a(\lambda)$ calculated from Eq. (4) are then corrected for water absorption: $\mu_a^w(\lambda) = \mu_a(\lambda) - C_{\mathrm{water}}\mu_{\mathrm{water}}(\lambda)$. We assumed a value of 0.3 for the water fraction in breast tissue (C_{water}).[5,10,11]

To determine the oxy- (HbO_2) and deoxyhemoglobin (HbR) concentrations, we assume that $\mu_a^w(\lambda) = C_{HbO_2}\mu_{a,HbO_2}(\lambda) + C_{HbR}\mu_{a,HbR}(\lambda)$, or in matrix form:

$$\mu_a^w = \boldsymbol{\mu}_{a,\mathbf{Hb}}\mathbf{C}, \tag{6}$$

where $\mu_a^w = (\mu_a^w, \lambda_{min}; \ldots; \mu_a^w, \lambda_{max})$ is the vector containing the water-corrected absorption coefficient values, $C = (c_{HbO_2}, c_{HbR})$ is a vector reflecting the concentration of the hemoglobin species, and $\boldsymbol{\mu}_{\mathbf{a,Hb}} = (\mu_{a,HbO_2,\lambda\ min}, \mu_{a,HbR,\lambda\ min}; \ldots; \mu_{a,HbO_2,\lambda\ max}, \mu_{a,HbR,\lambda\ max})$ is a matrix containing the absorption spectra of the hemoglobin species at the measurement wavelengths. Finally, by inverting Eq. (6) we obtain:

$$\mathrm{C} = (\boldsymbol{\mu}_{\mathbf{a,Hb}}^{\mathrm{T}} * \boldsymbol{\mu}_{\mathbf{a,Hb}})^{-1} * \boldsymbol{\mu}_{\mathbf{a,Hb}}^{\mathrm{T}} * \mu_a^w. \tag{7}$$

2.4 *Oxygen Consumption and Blood Flow Estimation*

Every molecule of hemoglobin carries four molecules of oxygen, thus a mass balance for oxygenated hemoglobin (HbO_2) within the measurement volume can be written as follows:

$$\frac{dN_{HbO_2}}{dt} = -\frac{OC}{4} + F[\mathrm{HbT}]_{blood}S_{a,O_2} - F[\mathrm{Hbt}]_{blood}S_{v,O_2}, \tag{8}$$

where N_{HbO_2} is the molar amount of oxygenated hemoglobin inside the measurement volume, OC is the oxygen consumption (in moles O_2/second) within the measurement volume, F is the volumetric blood flow into the measurement volume (in L/second), $[\mathrm{HbT}]_{blood}$ is the total blood hemoglobin concentration in the bood circulating through the tissue (i.e., as opposed to $[\mathrm{HbT}]_{tissue}$ which is the total hemoglobin concentration in the entire tissue volume sampled by the diffuse photons), S_{a,O_2} is the oxygen saturation of arterial blood (incoming), and S_{v,O_2} is the oxygen saturation of venous blood (outgoing). Here we assumed that blood inflow is equal to blood outflow (i.e., constant blood volume—this assumption is not always valid, but it applies to a significant number of our measurements). Dividing Eq. (8) by the tissue volume sampled by the spectrometer V_{tissue}, we obtain:

$$\frac{d[\mathrm{HbO_2}]}{dt} = -\frac{OC}{4V_{tissue}} + \frac{F}{V_{tissue}}[\mathrm{HbT}]_{blood}(S_{a,O_2} - S_{v,O_2}). \tag{9}$$

Assuming the measured tissue oxygen saturation SO_2 ($=[\mathrm{HbO_2}]/[\mathrm{HbT}]_{tissue}$) is the average of S_{a,O_2} and S_{v,O_2}, and further noting that $[\mathrm{HbT}]_{tissue}$ remains constant, we can rewrite Eq. (9) as:

$$\frac{dSO_2}{dt} = -\frac{OC}{4[\mathrm{HbT}]_{tissue}V_{tissue}} + \frac{2F_{blood}}{V_{tissue}}\frac{[\mathrm{HbT}]_{blood}}{[\mathrm{HbT}]_{tissue}}(S_{a,O_2} - SO_2). \tag{10}$$

The general solution to Eq. (10) is:

Table 1 Changes in total hemoglobin concentration averaged over all measurements. Only five subjects tested at 12 lbs of force.

Compression (lbs)	Relative blood volume change	Standard deviation
0→3	−13.5%	10%
3→6	−3.9%	4%
6→12	~−5%	(Insufficient samples)

$$SO_2(t) = C\exp\left(-\frac{2F_{blood}[\mathrm{HbT}]_{blood}}{[\mathrm{HbT}]_{tissue}V_{tissue}}t\right) - \frac{OC}{8F_{blood}[\mathrm{HbT}]_{blood}} + S_{a,O_2}, \tag{11}$$

where C is an integration constant. Subject to the initial condition that $SO_2(t=0)$ is equal to the measured tissue SO_2 at $t=0$ ($SO_{2,init}$), the particular solution to Eq. (10) can be written as:

$$SO_2(t) = S_{a,O_2} - \frac{(OC/V_{tissue})}{8(F_{blood}/V_{tissue})[\mathrm{HbT}]_{blood}} + \left(SO_{2,init} - S_{a,O_2} + \frac{(OC/V_{tissue})}{8(F_{blood}/V_{tissue})[\mathrm{HbT}]_{blood}}\right) \times \exp\left(-\frac{2F_{blood}[\mathrm{HbT}]_{blood}}{V_{tissue}[\mathrm{HbT}]_{tissue}}t\right). \tag{12}$$

By fitting Eq. (12) to time-resolved tissue oxygenation measurements, the parameters (OC/V_{tissue}) and (F_{blood}/V_{tissue}) can be estimated (oxygen consumption and blood flow per unit tissue volume). Before this can be accomplished, however, assumptions for the values of S_{a,O_2} and $[\mathrm{HbT}]_{blood}$ need to be made. In our analysis, we assumed $S_{a,O_2} = 0.98$, which is generally regarded as a normal value for arterial blood oxygenation in a healthy person. The choice of a value for $[\mathrm{HbT}]_{blood}$ is more complex. Normal systemic hemoglobin concentration values are 120 to 160 g/L for females.[12] However, the blood in the region probed by our spectrometer is dominantly contained in capillary vessels, whose hematocrit values are known to be 2 to 5 times lower than the systemic hematocrit[13] (due to the Fahraeus effect). For the purposes of this study, we assumed a value of 140 g/L for systemic hemoglobin concentration and a three times dilution factor in the capillaries, resulting in a value of 0.72 mM for $[\mathrm{HbT}]_{blood}$.

3 Results

Figure 3 shows a representative recording of the total hemoglobin content acquired during two consecutive compression cycles for a 30 year old woman with a body mass index (BMI) of 25. The shading in the figure indicates the force plateaus. There is a notable drop in total hemoglobin concentration, most of which occurs in going from 0 to 3 lbs of force. As shown in Table 1, when averaged over the entire patient set, a drop of 13.5±10% in HbT (mean ± standard deviation) is noted to correspond to applying 3 lbs of force,

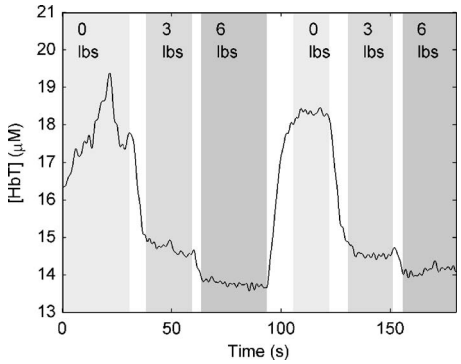

Fig. 3 Sample total hemoglobin concentration ([HbT]) recording. The shading indicates the compression plateaus. The [HbT] decreases proportionally to the amount of force applied.

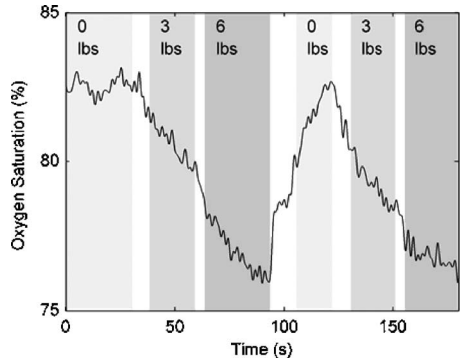

Fig. 5 Hemoglobin oxygen saturation (SO_2) recording. SO_2 decreases during compression due to reduced blood flow in the presence of sustained tissue oxygen consumption.

with a further drop of 3.9±4% resulting from increasing compression to the 6-lb level. For five subjects that agreed to be tested at 12 lbs of compression, an extra 5% decrease in HbT was observed in going from 6 to 12 lbs of force.

Figure 4 shows a total hemoglobin recording illustrating another physiological effect of breast compression: hyperemia. As can be seen in the figure, upon releasing compression after the first cycle, [HbT] does not simply return to the baseline level but rather significantly exceeds it. The overshoot in [HbT] continues to increase in later cycles and in the end stabilizes at approximately 25% beyond the initial baseline [HbT]. This hyperemic effect was observed in 35% of the subjects, with an average HbT overshoot of 11%.

Figure 5 shows a time-resolved measurement of the hemoglobin oxygen saturation for the same subject as Fig. 3. While SO_2 is relatively constant when no pressure is applied, it decreases during the compression plateaus, suggesting blood flow has been at least partially occluded and the tissue oxygen consumption exceeds oxygen delivery. Upon compression relief, SO_2 returns to the precompression value, but does so more slowly than the recovery in HbT levels.

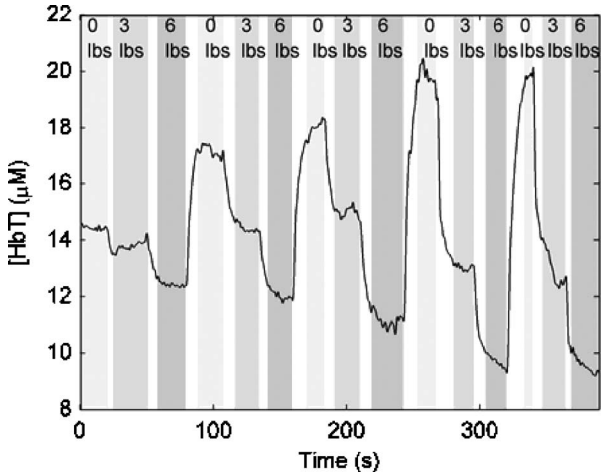

Fig. 4 Example of reactive hyperemia during repeated compression cycles. The shading indicates the compression force. The peak total hemoglobin content increases from cycle 1 through cycle 4, then plateaus.

As shown in Fig. 6, optical scattering also changes during breast compression and generally mimics the changes in [HbT], suggesting a correlation between the two physiological parameters.

Finally, we used the time-resolved SO_2 profile from the 6-lbs compression step for ten subjects where the compression plateau lasted for 90 s to estimate the volume-normalized blood flow and oxygen consumption. Figure 7 shows an example fit to the measured $SO_2(t)$ profile using Eq. (11). The small oscillations in SO_2 are probably artifacts caused by the cardiac cycle and serve as proof that blood flow has not ceased due to compression. Table 2 summarizes the oxygen consumption and blood flow findings. Average blood flow was 1.64±0.6 mL/100 mL/min, while average oxygen consumption was 1.97±0.6 μmol/100 mL/min.

4 Discussion

In the past, concerns have been raised that optical imaging under mammographic compression might be affected by depletion of the blood in breast tissues. From our results we can estimate that at least 50 to 70% of the initial blood volume should still be present in tissue at mammographic compression (20 lbs), which should allow for effective optical tomography. In fact, we could speculate that a higher percentage of the blood volume would be retained inside a tumor in comparison with the surrounding tissue because of the higher

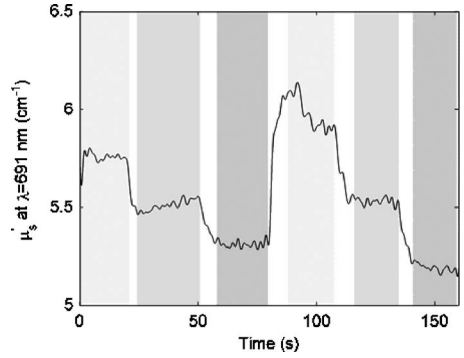

Fig. 6 Recording of the reduced scattering coefficient (μ_s') at λ =691 nm. The shading indicates the compression force. μ_s' decreases during compression.

Table 2 Volume normalized blood flow and oxygen consumption for ten subjects during 90-s, 6 lbs compression plateaus.

Subject	Blood flow (mL/100 mL/min)	Oxygen consumption (μmol/100 mL/min)
1	1.41	1.90
2	2.38	2.31
3	2.83	2.71
4	0.64	0.75
5	1.90	2.52
6	1.80	2.24
7	1.51	2.34
8	1.00	1.17
9	1.58	2.09
10	1.35	1.63
Average	1.64	1.97
Standard deviation	0.64	0.62

interstitial pressure of malignant lesions;[14] thus compression could actually enhance the tumor/normal tissue contrast.

A hyperemic effect was noted in many of the subjects, in which the total hemoglobin concentration rose above its initial level on release of compression. Only very weak correlations could be found between the strength of the hyperemic effect and the subject's body mass index, age, or day of menstrual cycle, but it is possible that the strength or time scale of hyperemia will be different in the presence of tumors/lesions.

As mentioned in the previous section, the hemoglobin oxygen saturation steadily decreases in all subjects during the compression plateaus. By modeling this decrease for the simplified case of constant $[\mathrm{HbT}]_{\mathrm{tissue}}$, we were able to obtain quantitative measures for the normalized blood flow (1.64 ± 0.6 mL/100 mL/min) and oxygen consumption (1.97 ± 0.6 μmol/100 mL/min) within the measurement volume. To our knowledge, these are the first absolute measurements of breast tissue oxygen consumption (OC) and volumetric blood flow (BF) by optical methods. Beaney et al.[15] have measured the regional blood flow and oxygen consumption in patients with breast carcinoma by means of the oxygen-15 steady-state inhalation technique and positron emission tomography (PET). They noted an average BF of 3.96 mL/100 mL/min and an average OC of 0.45 mL O_2/100 mL/min=19.8 μmol/100 mL/min for normal breast tissue. Another PET study by Wilson et al.[16] reported an estimated blood flow of 5.6 mL/100 mL/min. Our values are approximately three and ten times lower, respectively, for BF and OC. We believe most of the difference is explained by the difference in measurement geometry—the PET study measured the more metabolically active central area of the breast, while our measurements are limited to the most superficial 1 cm of tissue, where a significant fat content

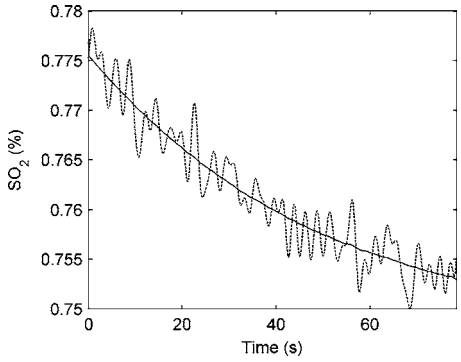

Fig. 7 Sample $SO_2(t)$ fit using Eq. (11). The solid line is the model prediction, while the dotted line is the experimental SO_2 recording. The small oscillation in SO_2 is probably caused by the cardiac cycle.

leads to lower oxygen consumption estimates,[17] while at the same time the compression applied to the tissue has lead to decreased blood flow. It is worth noting that in the PET study, breast tumors were found to have 4.7 times higher BF and 1.5 times higher OC than normal breast tissue. This leads us to believe that the tissue metabolic state will prove to be a highly specific marker for breast cancer.

As shown in Fig. 8, from the optical scattering measurements a certain degree of correlation ($R^2=0.45$) has been found between the change in μ_s' and the change in the total hemoglobin concentration. However, the data suggest a change of 0.12 cm^{-1} in μ_s' for every μM of HbT, which in turn would indicate that blood is responsible for approximately half of the tissue scattering. This is not realistic and in fact is contradicted by previously published results.[18] Therefore, other tissue components that co-vary with HbT during compression must account for the additional scattering changes, such as water and lipid concentration. To quantify changes in these components, the wavelength range of our spectroscopic system needs to be extended further into the infrared, a future focus for our work.

5 Conclusions

We show that breast compression leads to changes in the total hemoglobin content as well as hemoglobin oxygen saturation and tissue scattering. From the steady decrease in hemoglobin

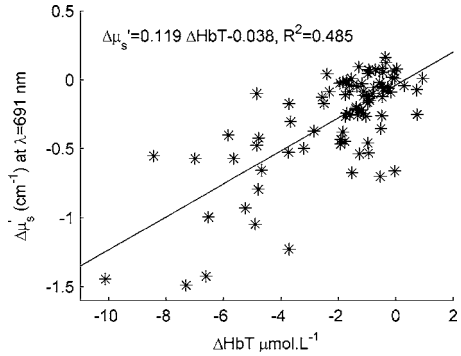

Fig. 8 Correlation between changes in [HbT] and μ_s'. The solid line indicates the linear fit, while the star (*) symbols indicate individual measurements.

saturation observed during compression plateaus, we are able to extract quantitative estimates of the tissue metabolic state that have the potential to aid cancer detection. While changes in breast optical properties during compression are significant, we do not expect them to impede tomographic optical imaging once taken into account. Furthermore, the compression-induced dynamic features of the optical/physiological property changes as well as the tissue oxygen consumption will likely be different in the presence of cancer pathology and should provide useful diagnostic information.

Acknowledgments

We acknowledge Dana Brooks and Dibo Ntuba for useful discussions, as well as funding under the National Institutes of Health (NIH) grants R01-CA97305 and U54-CA105480.

References

1. B. W. Pogue, S. P. Poplack, T. O. McBride, W. A. Wells, K. S. Osterman, U. L. Osterberg, and K. D. Paulsen, "Quantitative hemoglobin tomography with diffuse near-infrared spectroscopy: pilot results in the breast," *Radiology* **218**, 261–266 (2001).
2. J. C. Hebden, H. Veenstra, H. Dehghani, E. M. C. Hillman, M. Schweiger, S. R. Arridge, and D. T. Delpy, "Three-dimensional time-resolved optical tomography of a conical breast phantom," *Appl. Opt.* **40**, 3278–3287 (2001).
3. H. Jiang, Y. Xu, N. Iftimia, J. Eggert, K. Klove, L. Baron, and L. Fajardo, "Three-dimensional optical tomographic imaging of breast in a human subject," *IEEE Trans. Med. Imaging* **20**, 1334–1340 (2001).
4. R. Barbour, H. Graber, Y. Pei, S. Zhong, and C. Schmitz, "Optical tomographic imaging of dynamic features of dense scattering media," *J. Opt. Soc. Am. A* **18**, 3018–3036 (2001).
5. N. Shah, A. E. Cerussi, D. Jakubowski, D. Hsiang, J. Butler, and B. J. Tromberg, "The role of diffuse optical spectroscopy in the clinical management of breast cancer," *Dis. Markers* **19**, 95–105 (2003, 2004).
6. Q. Zhang, T. J. Brukilacchio, A. Li, J. J. Stott, T. Chaves, T. Wu, M. Chorlton, E. Rafferty, R. H. Moore, D. B. Kopans, and D. A. Boas, "Coregistered tomographic x-ray and optical breast imaging: initial results," *J. Biomed. Opt.* **10**, 024033 (2005).
7. S. D. Jiang, B. W. Pogue, K. D. Paulsen, C. Kogel, and S. P. Poplack, "In vivo near-infrared spectral detection of pressure-induced changes in breast tissue," *Opt. Lett.* **28**, 1212–1214 (2003).
8. S. Fantini, M. A. Franceschini, J. B. Fishkin, B. Barbieri, and E. Gratton, "Quantitative determination of the absorption spectra of chromophores in scattering media: a light-emitting-diode based technique," *Appl. Opt.* **33**, 5204–5213 (1994).
9. S. Fantini, M. A. Franceschini, and E. Gratton, "Semi-infinite-geometry boundary problem for light migration in highly scattering media: a frequency-domain study in the diffusion approximation," *J. Opt. Soc. Am. B* **11**, 2128–2138 (1994).
10. D. R. White, H. Q. Woodard, and S. M. Hammond, "Average soft-tissue and bone models for use in radiation dosimetry," *Br. J. Radiol.* **60**, 907–913 (1987).
11. H. Q. Woodard and D. R. White, "The composition of body tissues," *Br. J. Radiol.* **59**, 1209–1219 (1986).
12. R. Berkow, M. H. Beers, R. M. Bogin, and A. J. Fletcher, "Common medical tests," in *The Merck Manual of Medical Information (Home Edition)*, pp. 1375–1376, Merck Research Laboratories, Whitehouse Station, NJ (1997).
13. C. Desjardins and B. R. Duling, "Microvessel hematocrit: measurement and implications for capillary oxygen transport," *Am. J. Physiol. Heart Circ. Physiol.* **252**(3), H494–H503 (1987).
14. S. D. Nathanson and L. Nelson, "Interstitial fluid pressure in breast-cancer, benign breast conditions, and breast parenchyma," *Ann. Surg. Oncol.* **1**(4), 333–338 (1994).
15. R. P. Beaney, A. A. Lammertsma, T. Jones, C. G. McKenzie, and K. E. Halnan, "Positron emission tomography for in-vivo measurement of regional blood flow, oxygen utilisation, and blood volume in patients with breast carcinoma," *Lancet* **8369**(1), 131–134 (1984).
16. C. B. J. H. Wilson, A. A. Lammertsma, C. G. McKenzie, K. Sikora, and T. Jones, "Measurements of blood-flow and exchanging water space in breast-tumors using positron emission tomography—a rapid and noninvasive dynamic method," *Cancer Res.* **52**(6), 1592–1597 (1992).
17. M. Niwayama, T. Hamaoka, L. Lin, J. Shao, N. Kudo, C. Katoh, and K. Yamamoto, "Quantitative muscle oxygenation measurement using NIRS with correction for the influence of a fat layer: comparison of oxygen consumption rates with measurements by other techniques," *Proc. SPIE* **3910**, 256–265 (2000).
18. L. A. Paunescu, A. Michalos, J. H. Choi, U. Wolf, M. Wolf, and E. Gratton, "*In vitro* correlation between reduced scattering coefficient and hemoglobin concentration of human blood determined by near-infrared spectroscopy," *Proc. SPIE* **4250**, 319–326 (2001).